

November 01, 1979

Current-density distribution in solid-rotor induction motor

Mulukutla S. Sarma
Northeastern University

Recommended Citation

Sarma, Mulukutla S., "Current-density distribution in solid-rotor induction motor" (1979). *Electrical and Computer Engineering Faculty Publications*. Paper 9. <http://hdl.handle.net/2047/d20003733>

This work is available open access, hosted by Northeastern University.

CURRENT-DENSITY DISTRIBUTION IN SOLID-ROTOR INDUCTION MOTOR

Mulukutla S. Sarma
Department of Electrical Engineering
Northeastern University
Boston, MA 02115

ABSTRACT

The interaction between the eddy currents induced in the solid cylindrical rotor steel structure and the revolving field of the airgap produces the electrodynamic torque. The polyphase induction machine with solid-iron rotor offers advantages in ease of manufacture, in high torque per ampere at standstill, in withstanding high rotational stresses, and in operating in unusual environments. It is the purpose of this paper to present an approximate three-dimensional nonlinear numerical analysis of the solid-rotor induction motor for finding the three-dimensional current-density distribution in the solid rotor, in order to calculate the performance characteristics, based on finite-difference iterative techniques.

INTRODUCTION

The most elementary type of rotor for the polyphase induction machine is the solid iron rotor. There has been wide interest in the possible use of such solid-rotor motors for ultra high-speed inverter drives with suitable high stator supply frequency as well as variable speed drives for conventional frequencies and speed ranges. Some characteristics of the solid rotor machine are particularly suitable for solid-state power controls. Operational and military requirements demand very efficient, small, light-weight electrical power equipment. Conventional induction machine theory has proven inadequate for the solid-rotor induction motors, and the need has arisen for improved methods of investigation. A number of analytical methods of analysis¹⁻⁶ have been developed. Numerical methods^{5,7} of analysis have also been explored in two dimensions, while taking into account the field-dependent rotor magnetic permeability. An approximate three-dimensional nonlinear numerical analysis of the solid-rotor induction motor is presented in this paper.

ASSUMPTIONS

It is assumed that the axial component of the flux density B_z is zero everywhere in the entire region of the mathematical model. The justification for this step stems from the analysis of the three-dimensional linear

solution, and from the fact that the axial component of the flux density is indeed small and exists only in a small portion of the end of the rotor. As a consequence of this assumption, the problem can be posed in terms of the axial component of the vector potential A_z only, while setting the radial and tangential components of the vector potential, A_x and A_y , equal to zero in the entire region.

Only one pole pitch is considered in the analysis, as the solution is periodic in the peripheral direction. The curvature of the rotor and stator will not be considered, so that a Cartesian coordinate system can be used. The permeability of the stator stampings is assumed to be infinite. The stator currents are replaced by a surface current sheet in order to approximately match the constant voltage operation of the motor. The airgap of the model is assumed to be zero because it is easy to correct later for this assumption when computing the performance characteristics of the motor. The effect of the stator end windings as well as the end regions is not considered here, and the analysis is terminated at the end of the rotor surface in the axial direction.

Only one part of the rotor half will be investigated. In order to use less computer storage and time, the solution of the two-dimensional nonlinear problems is assumed at a fixed boundary located at a convenient distance from the rotor end. At a certain rotor depth, all the vector potentials are set according to the two-dimensional linear solution and are treated as fixed. This rotor depth in the radial direction is chosen for each value of slip in accordance with the results of the two-dimensional solutions.

All materials are taken to be isotropic and homogeneous. The conductivity of the rotor material is taken to be a constant. The permeability of the ferromagnetic materials μ is taken to be a single valued function of the magnetic induction B . The magnetization curve has been represented in a piecewise linear fashion for computer use. The dielectric effects are neglected. The rationalized MKSA system of units has been used throughout unless otherwise specified.

MATHEMATICAL MODEL

The mathematical model that is chosen for the analysis of the solid-rotor induction motor is shown in Figure 1. Referring to Fig. 1, one plane of the coordinate system is taken along the axis of the solid-rotor induction motor. The bore periphery represents the y axis and the x axis is radial. The coordinate system is fixed with respect to the rotating field, and its origin is conveniently located at a point 0, as shown in the figure. The partial differential equations are developed

first in terms of general space coordinates x , y , z , and time t , fixed to the medium under consideration, and are then transformed to a system fixed with respect to the rotating field.

THREE-DIMENSIONAL NONLINEAR VECTOR FIELD EQUATIONS IN CARTESIAN COORDINATES

For material regions which are void of electric charge and impressed current densities, but in which conduction current densities exist due to induction phenomena, the relevant Maxwell's equations in differential form are given as follows:

$$\nabla \times \bar{H} = \bar{J} \quad (1)$$

$$\nabla \cdot \bar{B} = 0 \quad (2)$$

$$\nabla \times \bar{E} = -\partial \bar{B} / \partial t. \quad (3)$$

The constituent relations are given by

$$\bar{B} = \mu \bar{H} \quad (4)$$

$$\bar{J} = \sigma \bar{E} \quad (5)$$

where μ is permeability and σ conductivity. In terms of a magnetic vector potential, one can write

$$\bar{B} = \nabla \times \bar{A} \quad (6)$$

$$\bar{E} = -\partial \bar{A} / \partial t - \nabla \phi \quad (7)$$

where ϕ is an electric scalar potential. Defining the reluctivity, v , as the reciprocal of the magnetic permeability μ , one can obtain

$$\nabla \times [v(\nabla \times \bar{A})] = -\sigma[\partial \bar{A} / \partial t + \nabla \phi]. \quad (8)$$

The scalar potential ϕ has to satisfy the following equation:

$$\nabla^2 \phi = -(\partial / \partial t)(\nabla \cdot \bar{A}) \quad (9)$$

which is a consequence of (8). With the assumption that the vector potential has only one component A_z , the subscript z of A_z may now be dropped, so that

$$\bar{A} = a_z A_z = a_z A. \quad (10)$$

Equation (8) yields coupled component partial differential equations. Uncoupling is achieved through appropriate arbitrary definitions of divergence of \bar{A} and the

gradient of ϕ . By defining

$$-\sigma(\partial\phi/\partial x) = (\partial/\partial z)[v(\partial A/\partial x)] \quad (11)$$

$$-\sigma(\partial\phi/\partial y) = (\partial/\partial z)[v(\partial A/\partial y)] \quad (12)$$

$$-\sigma(\partial\phi/\partial z) = (\partial/\partial z)[v(\partial A/\partial z)] \quad (13)$$

the following partial differential equation can be obtained for the description of the fields:

$$\begin{aligned} &(\partial/\partial x)[v(\partial A/\partial x)] + (\partial/\partial y)[v(\partial A/\partial y)] \\ &+ (\partial/\partial z)[v(\partial A/\partial z)] = \sigma(\partial A/\partial t). \end{aligned} \quad (14)$$

The components of the flux density and of the electric field intensity may simply be evaluated in terms of A as follows:

$$B_x = \partial A/\partial y \quad (15)$$

$$B_y = -\partial A/\partial x \quad (16)$$

$$B_z = 0 \quad (17)$$

$$E_x = \sigma^{-1}(\partial/\partial z)[v(\partial A/\partial x)] \quad (18)$$

$$E_y = \sigma^{-1}(\partial/\partial z)[v(\partial A/\partial y)] \quad (19)$$

$$E_z = -\partial A/\partial t + \sigma^{-1}(\partial/\partial z)[v(\partial A/\partial z)]. \quad (20)$$

So far, the equations have been developed in terms of a coordinate system fixed to either the stator or rotor. In order to eliminate the time coordinate in the equations, a coordinate transformation will be performed, so that the new coordinate system will be stationary with respect to the rotating field. The following transformation equations are

$$x = x_s = x_r \quad (21)$$

$$z = z_s = z_r \quad (22)$$

$$y = (\pi/\tau)y_s - \omega t_s = (\pi/\tau)y_r - S\omega t_r \quad (23)$$

where S is the per-unit slip; ω is stator supply angular frequency; τ is the pole pitch; and the subscripts s and r refer to stator and rotor, respectively. The partial differential equations are then transformed to the following.

$$\text{In the airgap:} \quad (24)$$

$$\partial^2 A^{(a)}/\partial x^2 + (\pi^2/\tau^2)[\partial^2 A^{(a)}/\partial y^2] + \partial^2 A^{(a)}/\partial z^2 = 0.$$

In the linear region of the rotor.

$$\begin{aligned} \partial^2 A^{(r)} / \partial x^2 + (\pi^2 / \tau^2) \partial^2 A^{(r)} / \partial y^2 + \partial^2 A^{(r)} / \partial z^2 \\ + S\omega \mu \sigma \partial A^{(r)} / \partial y = 0. \end{aligned} \quad (25)$$

In the nonlinear region of the rotor:

$$\begin{aligned} (\partial / \partial x) \{v[\partial A^{(r)} / \partial x]\} + (\pi^2 / \tau^2) (\partial / \partial y) \{v[\partial A^{(r)} / \partial y]\} \\ + (\partial / \partial z) \{v[\partial A^{(r)} / \partial z]\} = -S\omega \sigma [\partial A^{(r)} / \partial y]. \end{aligned} \quad (26)$$

The field components, in the interior of the rotor, will transform as follows:

$$B_x = (\pi / \tau) (\partial A / \partial y) \quad (27)$$

$$B_y = -\partial A / \partial x \quad (28)$$

$$B_z = 0 \quad (29)$$

$$E_x = \sigma^{-1} (\partial / \partial z) [v(\partial A / \partial x)] \quad (30)$$

$$E_y = \sigma^{-1} (\pi / \tau) (\partial / \partial z) [v(\partial A / \partial y)] \quad (31)$$

$$E_z = S\omega (\partial A / \partial y) + \sigma^{-1} (\partial / \partial z) [v(\partial A / \partial z)]. \quad (32)$$

Knowing the \bar{E} -fields, the current-density fields are readily given by making use of Eq. (5). It may be noted that all the three components of the \bar{J} -field exist in spite of the assumption that the axial component of the \bar{B} -field is zero.

NUMERICAL ANALYSIS

A suitable fine lattice system is laid out on the mathematical model for numerical analysis. The number of lattice points and the region to be considered for sufficiently accurate results depend on the value of the slip. Partial differential equations are transformed into difference form for numerical work. The boundary conditions are then specified in differential and difference forms. The details, omitted here because of space limitations, are discussed in Reference 8. The periodicity condition is to be satisfied in the peripheral y direction. The z component of the current density must vanish at the rotor-end surface. The surface current sheet at the stator-rotor boundary surface is to be matched appropriately.

An iterative procedure is then developed for the numerical solution of the nonlinear partial differential equations. In each iteration, the vector potentials at each of the lattice points are calculated, using

reluctivities calculated during the previous iteration, by successive point relaxation method; later the reluctivities are recomputed using the newly calculated vector potentials and are underrelaxed. A new method of computing an appropriate relaxation factor for the reluctivity at each lattice point depending on its location on the magnetization characteristic has been successfully implemented. This method has resulted in some significant improvement in convergence. The adopted iterative scheme carries out the computations plane by plane (xy planes) along the positive z direction. Sweeping has been done in the positive y direction on a given line in the xy plane, then in a positive x direction, and then in the positive z direction on all the xy planes, thereby covering all the lattice points in the model. The convergence is judged by the fact that the algebraic sum of the residuals and the sum of the absolute values of residuals of the vector potential are monotonic functions and the sum is of the order of the average value of the vector potentials. Thus the average residual is of the order of less than 0.01 percent of the average vector potential. The number of iterations required for an acceptable convergence is of the order of 100 iterations for about 20,000 lattice points.

CONCLUDING REMARKS

A numerical method has been established here for finding the three-dimensional current density distribution in a solid rotor of high-speed induction motors in order to calculate the performance characteristics. It is only a first approximation, and further refinements are suggested in Reference 8. The method presented has been applied to analyze a 5-hp, 6-pole, 3200-Hz, three-phase, 145-V, star-connected solid-rotor induction machine. The computed results indicate the following characteristics: the end of the solid rotor of the induction motor is more and more saturated as the end surface is approached. The nonlinear portion increases continuously. The nonlinear depth at the end surface of the rotor is about twice that at the center of the rotor. The x and y components of the current densities become significant only in the last 1/20th part of the rotor. The z component of the current density is significant throughout, although it is zero right on the end surface of the rotor. The radial flux density shows a significant rise in the end part of the rotor.

The computer program is so developed that it can easily be modified for other values of slip. The dimensions X_b and Z_b of Fig. 1 need to be decided judiciously and a new convenient lattice system is to be chosen.

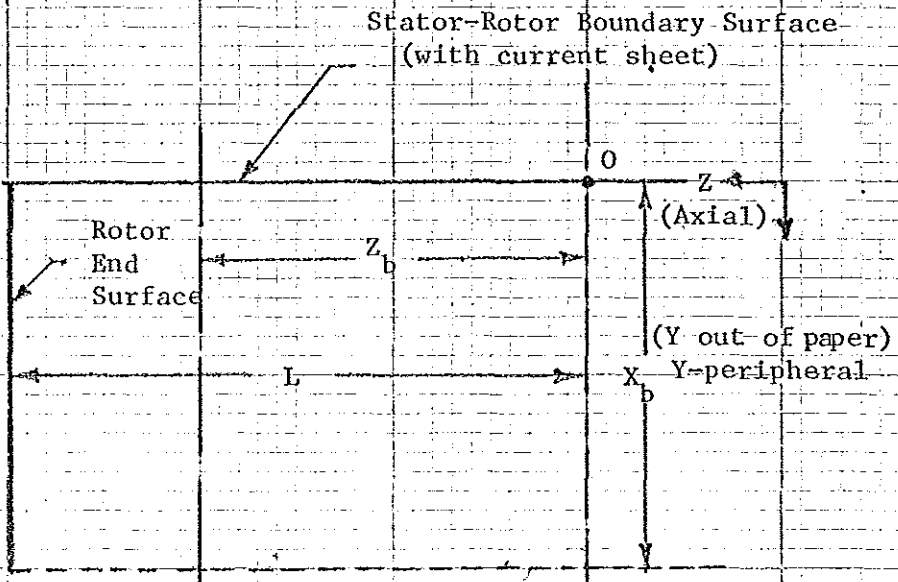
After satisfactory convergence, the current densities and flux densities at all the lattice points, as well as the torque and the terminal voltage are evaluated.

ACKNOWLEDGEMENTS

The author would like to express his sincere thanks to Prof. E. A. Erdelyi, Dr. J. C. Wilson, and Dr. A. L. Jokl for their helpful suggestions and discussions.

REFERENCES

1. H. M. McConnell and E. F. Sverdup, "The induction machine with solid iron rotor," AIEE Trans. Power App. Syst., vol. 74, pp. 343-349, June 1955.
2. A. J. Wood and C. Concordia, "An analysis of solid-rotor machines, pt. III: Finite length effects; pt. IV: An approximate nonlinear analysis," AIEE Trans. Power App. Syst., vol. 79, 1960.
3. L. A. Finzi and D. A. Paice, "Analysis of the solid iron rotor induction motor for solid-state speed controls," IEEE Trans. Power App. Syst., vol. PAS-87, pp. 590-596, Feb. 1968.
4. B. Heller and M. S. Sarma, "The electromagnetic field in solid iron," Acta Tech. (Prague), no. 6, 1968.
5. J. C. Wilson, "Theory of the solid-rotor induction machine," Ph.D. dissertation, Univ. Colorado, Boulder, 1969.
6. M. S. Sarma and G. R. Soni, "Solid-rotor and composite-rotor induction machines," IEEE Trans. Aerosp. Electron. Syst., vol. AES-8, pp. 147-155, Mar. 1972.
7. J. C. Wilson, E. A. Erdelyi, and R. E. Hopkins, "Aerospace composite-rotor induction motors," IEEE Trans. Aerosp. Electron. Syst. (Suppl.), vol. AES-3, June 1965.
8. M. S. Sarma and E. A. Erdelyi, "Synthesis of high speed homopolar alternators and theory of solid rotor electrical machines, phase DD, pt. IV," U.S. Army Mobility Equipment Research and Development Center, Fort Belvoir, Va., USAMERDC Rep., Mar. 1969.
9. M. S. Sarma and J. C. Wilson, "Accelerating the Magnetic Field Iterative Solutions", IEEE Trans. on Magnetics, vol. MAG-12, No. 6, pp. 1042-44, Nov. 1976.



Mathematical model of solid-rotor induction motor.

Figure 1.